



RESEARCH PAPER

OPEN ACCESS

Synthesis and characterization of TiO₂ nanoparticle infused with MMT for testing its antibacterial efficacy

CI. Anish, M. Jaya Rajan*

Department of Chemistry & Research, Annai Velankanni College, Tholayavattam

Manonmanium Sundarnar University Abishekapatti, Tirunelveli, Tamilnadu, India

Article published on November 13, 2023

Key words: TiO₂/MMT nanocomposite, Antibacterial activity, Optical properties, Photo stability, Nontoxicity

Abstract

Bio nanocomposite clay-based material Montmorillonite (MMT) and Titanium dioxide (TiO₂) are modified for the application to antibacterial effect in waste water. TiO₂ is employed because of its photostability, nontoxicity, high activity, and relatively low cost. In that view, the current study investigates the antibacterial potentials of TiO₂/MMT nanocomposite formed by the hydrothermal synthesis route. The physicochemical properties of the formed TiO₂/MMT nanocomposite were characterized by the powdered XRD, SEM, EDAX, BET, FTIR, and UV-Visible spectroscopies. The crystallinity and crystal structure are confirmed by the XRD, the bonding information and surface functionality by the FTIR, and the morphology and elemental composition with the SEM/EDAX analysis. From the BET investigations, the structural morphology of TiO₂/MMT nanocomposite showed an improved pore volume, surface area, and voids, while the optical properties of TiO₂ nanoparticles significantly enhanced following the composite formation with that of MMT. Further tests of antibacterial activity of TiO₂/MMT nanocomposite towards Gram-positive (*Bacillus cereus*, *Enterococcus* and *Staphylococcus aureus*) and Gram-negative (*Escheria coli* and *Pseudomonas aeruginosa*) bacteria supported the efficiency of prepared composite and thereby confirming its promising potentials in the applications related to microbial removal from wastewater.

*Corresponding Author: M. Jaya Rajan ✉ jayarajanm1983@gmail.com

Introduction

Water is a primary resource for the presence of life on earth and access to clean water is critical for humans and the ecosystem. Nonetheless, during the last decades water quality has been negatively influenced by a continuously increasing population, rapid industrialization, increasing urbanization, and careless utilization of natural resources (Vardhan *et al.*, 2019; Carolin *et al.*, 2017). Organic matter, nutrients, pharmaceutical and personal care products, poly- and per fluoro alkyl substances, biocides, heavy metals, dyes, radionuclides, plastics, nanoparticles and pathogens are among the pollutants of major concern (Villarín and Merel, 2020).

In recent years, there has been huge demand for the development of sustainable water treatment technologies due to a significant increase in the number of river and ground water pollutant bodies like the metallic, dye, and toxic ions (Kumar, 2021). Since the drinking and agriculture water contains large amounts of toxic substances and dyestuffs and it is of highest priority to remove them in order to overcome the water scarcity at a global level (Prasannamedha *et al.*, 2020). In addition to the separation of pollutants from the river and ground water streams, the uninformed microorganism purification is also highly important as the microbial contaminated water can cause severe health problems and may even drag to the death (Zeng *et al.*, 2019).

Titanium dioxide (TiO₂) is an important and most efficient semiconductor material which is commonly used as a photocatalyst by taking advantage of its photosensitizing capacity, i.e., as photo-oxidizer or reducer to breakdown/activate the organic, inorganic, and biological moieties (Rasouli *et al.*, 2014; Butman *et al.*, 2020). In addition, taking into consideration of its oxido reductase potentials under the influence of irradiation, the TiO₂ and its hybrid composites are being engaged for the controlling of the microbial contamination and disinfection of membrane/glass surfaces using chemical agents (biocides). Since the

recently developed semiconductor metal oxide photo catalysts are investigated to serve as promising alternatives to the conventional disinfection techniques, there have been many different composites introduced with change of ingredients and ionic composition in order to address multiple application requirements (Hassani *et al.*, 2020; Bayal *et al.*, 2017). As an example, the MMT (TiO₂-MMT) is commonly used as photocatalyst support due to its large surface area, cation absorption capacity. Montmorillonite is an effective dopant; it can influence the photocatalytic efficiency of Titania by decreasing the particle size and increasing its thermal stability and surface area. Modification of Montmorillonite will get improved antibacterial effect. This is because the MMT can easily attach to the cell wall of microbe (Nabih *et al.*, 2019; Ghanbari *et al.*, 2020).

Therefore, the present work investigates the efficiency of TiO₂/MMT nanocomposite synthesized by the hydrothermal method. For the characterization, the crystalline and crystal structure of the composite were evaluated by the powdered XRD analysis, while the optical and photo catalytic property by the UV-Vis, functionality by FTIR, morphology by SEM, and surface area with the BET analysis. Further, the antibacterial activity of as-synthesized TiO₂/MMT nanocomposite was evaluated by testing against the four different bacterial cultures of *Enterococcus faecalis* and *Staphylococcus aureus* (Gram-positive) and *Escheria coli* and *Pseudomonas aeruginosa* (Gram-negative), as the results generated can help to improve the quality of water following its treatment.

Material and methods

Chemicals

All chemicals such as titanium dioxide (TiO₂), Montmorillonite (MMT), titanium isopropoxide (TTIP) and methanol were purchased from Sigma Aldrich (Mumbai, India). It was used as received without further purification. Distilled water was used as solvent in all the preparations.

Synthesis of TiO₂/MMT nanocomposite

To synthesize TiO₂-MMT composites, Tetrabutyl titanate was added to deionized water of about 30 ml. Stir the mixture for 5 min so that the mixture gets a uniform dispersion. In a beaker 80 ml of deionized water was taken, Montmorillonite (MMT) was added to it. After a gentle mix beaker was sealed well with a clingfilm to avoid evaporation. This suspension was stirred using a magnetic stirrer for 4 hrs. Now the pH of the solution reaches at 8. Allow the solution to stand for 10 min so that it reaches homogeneity. Now transfer the solution to a hydrothermal autoclave and heat the mixture at 200°C for 12 hrs. Cool the mixture to room temperature. Wash the sample and kept at hot air oven for 12 hrs at 80°C to get TiO₂-MMT composites.

Instrumental analysis

The X-ray diffraction (XRD) pattern was recorded by using BrukerD8 advance powder XRD instrument with CuK α radiation ($\lambda = 1.5406\text{\AA}$). The optical properties by means of UV-Visible spectroscopy were tested on AGILENT 5000 UV-Vis spectrophotometer in the spectral range between 200 to 700nm. The FTIR analysis was recorded on the Thermo Nicolet Avatar 370 in the range of wave number is 4000 to 400cm⁻¹. The microstructure was recorded on the Jeol/JEM2100 with the point of resolution 0.23nm.

*Antibacterial activity assay**Test organism*

Enterococcus faecalis, Staphylococcus aureus, Escherichia coli, and Pseudomonas aeruginosa were the test organisms employed for the antimicrobial analysis, and they were bought from the Microbial Type Culture Collection and Gene Bank (MTCC) in Chandigarh. Nutrient Agar was used to sustain the bacterial strains.

Nutrient broth preparation

A NA plate was inoculated with pure culture from the plate, and it was subcultured at 37°C for 24 hours. To create the standardized inoculums, fresh culture was aseptically added to a 2 mL sterile 0.145 mol/L saline tube. Cell density was then adjusted to a 0.5

McFarland turbidity standard to produce a bacterial suspension with 1.5 $\times 10^8$ colony forming units (CFU)/ml.

Preparation of plates

According to the manufacturer's instructions, the medium is prepared and sterilised. For testing on fastidious organisms, de-fibrinated blood may be required; in this instance, the medium should chill to 50°C before 7% of blood is added. Since human blood might include antibacterial agents, it is not advised. Petri dishes should have the medium added to a depth of 1 mm, using 25 mL for an 85 mm circular dish and 60 ml for a 135 mm circular dish. After being prepared, the poured plates are kept at 4°C and utilized within a week.

The plates are dried with the lids slightly ajar before inoculation to ensure that there are no water droplets on the agar surface. The drying circumstances will determine how long it takes to do this. When the medium was being prepared, its pH was monitored and kept within the range of 7.2 to 7.4.

Preparation of inoculums

A wire loop was used to transfer at least four morphologically identical colonies from an agar medium to a test tube containing 1.5 mL of sterile appropriate broth. The tubes were incubated for 2 hours at 35-37°C to produce a moderately turbid bacterial solution. Dilution with sterile saline or broth at a density equivalent to the barium sulphate standard, 0.5 McFarland units, is used to standardize the density of the suspension. The standards were vigorously shaken before use.

Inoculation

To ensure that the density did not change, the plates were infected within 15 minutes of the suspension being prepared. A sterile cotton-wool swab was dipped into the solution, and excess was removed by rotating the swab against the edge of the tube above the fluid level. The medium was infected by streaking the swab evenly across the plate's surface in three directions.

Antibiotics discs

After drying, single discs are placed using forceps, a sharp needle, or a dispenser and gently pushed to achieve uniform contact with the medium. When testing fastidious organisms, use a loop to contact many colonies and cross streak the appropriate plate for uniform distribution. A maximum of six discs can be contained on an 85mm circular plate, and twelve discs can be easily accommodated on 135mm circular discs that can be stored at 4°C in sealed containers with a desiccant and allowed to reach room temperature before being opened. The discs must be used before the expiry date on the label, and the laboratory-prepared antimicrobial solution is used as follows:

1. Took a 2mm loop filled of standard antibiotic solution and carefully dropped it onto a wet paper disc until the moistened disc adhered to the loop.
2. Placed the wet disc on the surface of the infected plate in the suitably labelled segment (caution must be exercised to avoid accidental "contamination" of other discs in the Petri dish with the antibiotic solution).
3. Repeated the procedure for each antimicrobial agent to be employed, inserting the impregnated discs into their corresponding marked segments.

Incubation

For fastidious species, the microbial plates were incubated for 16 to 18 hours at 35 to 37°C aerobically or in a CO₂ environment.

Reading of zones of inhibition

Zone diameters were measured to the closest millimetre using vernier callipers or a thin transparent millimetre scale. The zone edge is defined as the point of sudden decrease in growth, which in most circumstances corresponds to the point of full inhibition of growth. In some batches of medium, organisms may form a film of growth within the sensitive zone, which can be ignored. Swarming *proteus* spp. has comparable results. Each zone size is evaluated by reference to the organism (Waran and Pp, 2016; Ranjbar *et al.*, 2016; Malkappa *et al.*, 2018).

Results and discussion

Physicochemical characterization

Fig. 1(a) provides the powdered XRD pattern of synthesized TiO₂/MMT nanocomposite where the analysis indicates the phase structure. Since Ti has an anatase phase, this is the most activated polymorph for the occurrence of photocatalytic process. In that way, the TiO₂/MMT nanocomposite shows the main peaks at the 2θ of 25.5°, 27, 35.5°, 42°, 54°, 56°, and 69° where they all can be indexed to the planes of 101, 004, 200, 105, 211, and 204 (respectively) and are corresponding to the anatase phase of TiO₂ (JCPDS 21-1272) (Yang and Liang, 2019; Parand *et al.*, 2020; Waran and Pp, 2016). Further, the crystalline size of TiO₂/MMT sample when calculated using Debye-Scherrer equation provided the average crystal size of 15nm, thereby confirming for the nanocrystalline nature of TiO₂/MMT sample. Thus, from the XRD analysis of TiO₂/MMT, it confirms the existence of anatase phase having the most suitable photocatalytic active phase of TiO₂ elements in the nanocomposite of TiO₂/MMT (Ruchianwar *et al.*, 2022; Joseph *et al.*, 2022).

Similarly, the FTIR analysis investigates the quality and chemical composition of as-synthesized TiO₂/MMT nanocomposite where the results are provided in Fig. 1(b) in the spectral range of 4000-400 cm⁻¹. From the spectrum, the observation of broad absorption bands centred at 3631 and 3336 cm⁻¹ are attributable to the O-H stretching and bending vibrations (respectively) (Van Hung *et al.*, 2021). It is worth mentioning here that the availability of such a hydroxyl group onto the surface of TiO₂/MMT nanocomposite, the photocatalyst nature and its overall efficiency can significantly be influenced. Also, the peak at 1664 associated with C=O stretching and 1086 cm⁻¹ corresponds to the stretching vibrations of C-O bonds of MMT moiety. The peak at 696 cm⁻¹ is related to the C=C bending. Additionally, the peaks at 566 and 485 cm⁻¹ correspond to the Ti-O and O-Ti-O absorption bands of TiO₂ respectively (Palhares *et al.*, 2021; Kadhim *et al.*, 2022).

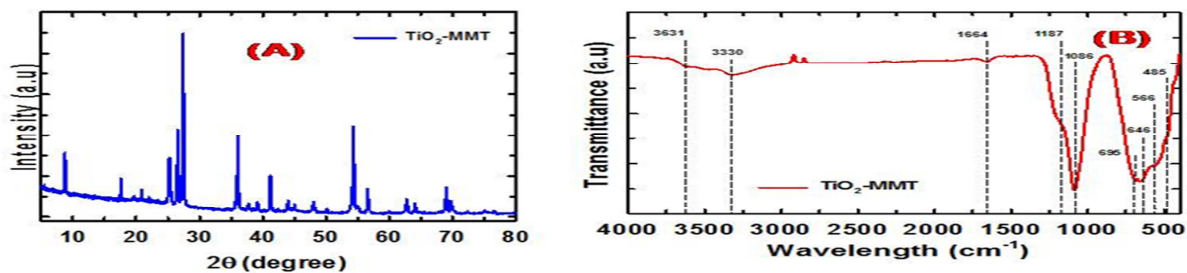


Fig. 1. Powdered XRD spectral pattern (a) and FTIR spectral analysis (b) of TiO₂/MMT nanocomposite.

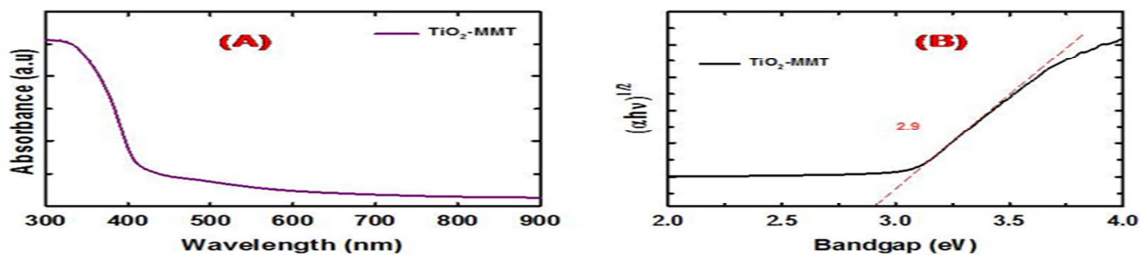


Fig. 2. (a) UV absorbance spectra and (b) band gap energy of TiO₂/ MMT nanocomposite.

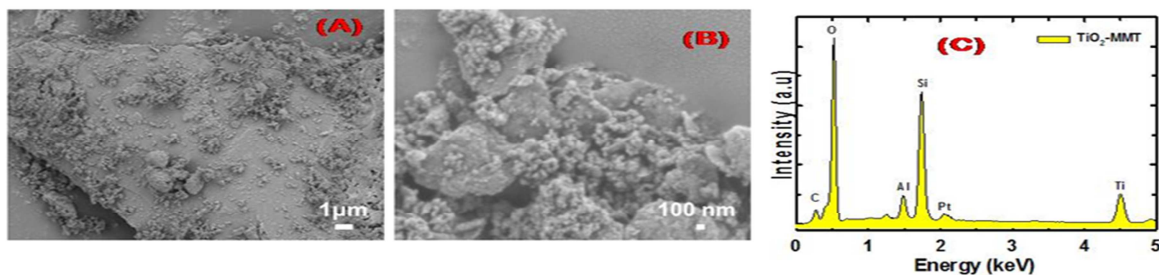


Fig. 3. SEM micrographs of TiO₂/MMT nanocomposite at different magnifications (A, B) and the corresponding EDAX spectra (C).

Fig. 2(a) provides the absorbance spectral analysis of TiO₂/MMT nanocomposite and from the spectrum, a very sharp band edge in the UV region of 300 to 400 nm is getting observed for the TiO₂/MMT nanocomposite. Relation between absorbance coefficient and energy is measured for TiO₂/MMT nanocomposite which is shown in Fig. 2(b). Since MMT has very wide band gap energy (E_g) which can restrict the photo reactivity of the material. However, TiO₂ has band gap energy (E_g) of 3.2 eV which lies in the ultraviolet region. Addition or coating of Titanium dioxide over MMT, the surface reduces the bandgap energy to the lower value 2.92 eV. This change can make the photo-excitation more adapted and respond to the ultraviolet region (Mahanta *et al.*, 2022; Eddy *et al.*, 2020). From the results obtained, due to the

covering of TiO₂ nanoparticles above MMT a strong quenching can be noticed. It also acts positively on removing and degradation of the pollutant easily from the organic dyes.

Surface morphology of the synthesized TiO₂/MMT was observed by SEM analysis. Figure 3(a-c) represents the SEM image of TiO₂/MMT at various magnifications. SEM images of TiO₂/MMT shows irregular size particles with no definite shape. The lumps with irregular sizes of silicon dioxide can be notice from the scanning electron micrographs. Granular structure of TiO₂ in an embedded form also is noticed. The presence of TiO₂ immobilized on MMT was confirmed from the SEM image by its appearance of white spots around the MMT surface.

The TiO₂/MMT samples show that MMT and TiO₂ forms overlapping of aggregates (Ting Wang *et al.*, 2021; Takari *et al.*, 2021; Jesus *et al.*, 2021).

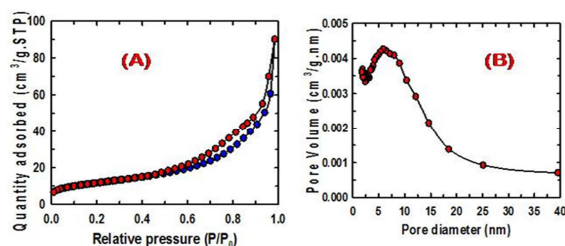


Fig. 4. (a) N₂ adsorption–desorption isotherms surface area and (B) corresponding pore size distribution of TiO₂/MMT nanocomposite.

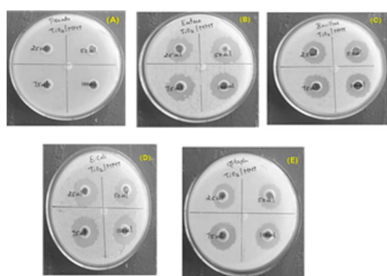


Fig. 5. Antibacterial activity of TiO₂/MMT nanocomposite (A) *Pseudomonas aeruginosa*, (B) *Enterococcus faecalis*, (C) *Bacillus cereus*, (D) *Escherichia coli*, and (E) *Staphylococcus aureus*.

Table 1. Pore size distribution of TiO₂/MMT nanocomposite.

Sample	SA (m ² /g)	Pore volume (cm ³ /g)	Pore size (nm)
TiO ₂ -MMT	42.32	0.139	5.92

Table 2. Inhibition zone of TiO₂/MMT nanocomposite

TiO ₂ /MMT	Inhibition zone (mm)				
	25µl	50µl	75µl	100µl	control
<i>Escherichia coli</i>	15mm	15mm	16mm	17mm	18mm
<i>Pseudomonas aeruginosa</i>	10mm	10mm	10mm	10mm	16mm
<i>Bacillus cereus</i>	18mm	15mm	16mm	18mm	21mm
<i>Staphylococcus aureus</i>	14mm	15mm	18mm	18mm	18mm
<i>Enterococcus faecalis</i>	21mm	20mm	21mm	20mm	22mm

The EDAX spectra of synthesized TiO₂/MMT nanocomposite are shown in Fig. 3(C). The characteristic peaks of Ti, Si, O and C can be observed in TiO₂/MMT sample. EDX analysis confirmed the

presence of Ti, Si, and O. The characteristic peak for Ti element was observed this indicates that the TiO₂ particles were well doped on the surface of MMT (Bilgic *et al.*, 2022).

BET analysis is carried out to determine the surface area of the synthesized TiO₂/MMT nanocomposite. Fig. 4(a-b) shows the N₂ adsorption–desorption isotherms and pore distribution curves of the synthesized TiO₂/MMT nanocomposite. The surface area, pore size and pore volume are shown in Table 1. The nitrogen sorption isotherms of TiO₂/MMT nanocomposite can be categorized as type IV isotherms with type H4 hysteresis loop. The hysteresis loop of TiO₂/MMT nanocomposite covers a relative pressure range of about 0.1–0.8. The quantity of N₂ adsorbed in the relative pressure range slowly increases gradually above 0.85, it rapidly increases to reach at 0.99 to obtain a maximum value. The mean pore diameter of TiO₂/MMT nanoparticle decreased while the surface area, micropore volume and total pore volume increased. This indicates that TiO₂ nanoparticles have entered into the MMT (YerliSoylu *et al.*, 2023; Palhares *et al.*, 2021).

Antibacterial activity

The antibacterial activity of synthesized TiO₂/MMT was evaluated against Gram-positive (*Enterococcus faecalis* and *Staphylococcus aureus*) and Gram-negative (*Escherichia coli* and *Pseudomonas aeruginosa*) bacterial cultures on Nutrient agar. To distribute the inoculums, the plates were swirled 2-3 times of bacteria by rotating the dish.

After inoculation, 1.5mg of the test samples were taken on the bacteria-seeded plates using sterile forceps and the plates were incubated for one day. This measured and registered the inhibition zone around the disks. Fig. 5 (A-D) provides the visual observation of inhibition zones indicating the antibacterial activity of TiO₂/MMT nanocomposite and the zone of inhibition values in mm are tabulated in Table 2. Erythromycin was used as the control to test against *Pseudomonas aeruginosa*, *Escherichia coli*, *Enterococcus*, *Bacillus* and *Staphylococcus aureus*.

From the analysis, both Gram negative and positive bacteria showed better antibacterial activity followed by the TiO₂/MMT nanocomposite treatment. In this, *Escherichia coli*, *Staphylococcus aureus*, *Bacillus*, *Enterococcus* and *Staphylococcus aureus* showed better activity due to the higher penetrating tendency to break the bacterial cell wall, while *Pseudomonas aeruginosa* showed the least activity because of the limited penetrating tendency against the bacterial cell wall (Daniel Sam *et al.*, 2021).

Conclusion

In this work, the TiO₂/MMT nanocomposite was successfully synthesized using the hydrothermal method. The surface morphology and BET confirms that the MMT nanoparticle is decorated on the surface of TiO₂. EDAX confirms the presence of elements and their purity. The FTIR confirms the absorption band of O- Ti- O. The XRD analysis of TiO₂/ MMT nanocomposite confirms the existence of the anatase phase, which is most suitable for the photocatalytic active phase using TiO₂. From UV-Vis spectra, the band gap of synthesized nanocomposite decreases and therefore the organic pollutant dyes can be degraded easily. In addition, the TiO₂/MMT showed better inhibition zones against gram-negative and gram-positive bacteria confirming the antibacterial activity. Finally, based on the photocatalytic dye degradation capacity and antibacterial activity, the synthesized TiO₂/MMT nanocomposite can serve as a promising material for treatment of dyestuffs and as an antibacterial agent.

References

Jesus AML, Ferreira AM, Lima LFS, Batista GF, Mambrini RV, Mohallem NDS. 2021. Micro-mesoporous TiO₂/SiO₂ nanocomposites: Sol-gel synthesis, characterization, and enhanced photodegradation of quinoline, *Ceramics International* **47(17)**, 23844-23850.

Takari A, Ghasemi AR, Hamadani M, Sarafrazi M, Najafidoust A. 2021. Molecular dynamics simulation and thermo-mechanical characterization for optimization of three-phase epoxy/TiO₂/SiO₂ nano-composites. *Polymer Testing* **93**, 106890.

Bilgic A. 2022. Fabrication of mono BODIPY-functionalized Fe₃O₄@SiO₂@TiO₂ nanoparticles for the photocatalytic degradation of rhodamine B under UV irradiation and the detection and removal of Cu(II) ions in aqueous solutions, *Journal of Alloys Compounds* **899**, 163360.

Bayal N, Singh R, Polshettiwar V. 2017. Nanostructured Silica-Titania Hybrid using Fibrous Nanosilica as Photocatalysts. *Chemical Sustainable Chemistry* **10(10)**, 2182-2191.

Butman MF, Gushchin AA, Ovchinnikov NL, Gusev GI, Zinenko NV, Karamysheva SP, Krämer KW. 2020. Synergistic Effect of Dielectric Barrier Discharge Plasma and TiO₂-Pillared Montmorillonite on the Degradation of Rhodamine B in an Aqueous Solution. *Catalysts* **10**, 359.

Carolin CF, Kumar PS, Saravanan A, Joshiba GJ, Naushad M. 2017. Efficient techniques for the removal of toxic heavy metals from aquatic environment: A review, *Journal of Environmental Chemical Engineering* **5(3)**, 2017,

Pragathiswaran C, Smitha C, Abubakkar BM, Govindhan P, Krishnan NA. 2021. Synthesis and characterization of TiO₂/ZnO-Ag nanocomposite for photocatalytic degradation of dyes and anti-microbial activity, *Materials Today: Proceedings*, 3357-3364.

Daniel Sam N, Anish CI, Sabeena G, Rajadurai S, Gandhimathi S, Annadurai G, Jaya Rajan M. 2021. Synthesis and Characterization of TiO₂-CeO₂ (TiO₂-Ce) Nanocomposite: Testing its antibacterial effect, *Research Journal of Chemistry and Environment* **25(10)**, 13-19.

Kadhim FJ, Hammadi OA, Muthesher NH. 2022. Photocatalytic activity of TiO₂/SiO₂ nanocomposites synthesized by reactive magnetron sputtering technique, *Journal of Nanophotonics* **16(2)**, 026005.

- Ghanbari S, Givianrad MH, Aberoom, Azar P.** 2020. Synthesis and characterization of visible light-driven N-Fe-co-doped TiO₂/SiO₂ for simultaneous photo removal of Cr (VI) and AZO dyes in a novel fixed bed continuous flow photoreactor, Canadian Journal of Chemical Engineering **98**, 705–716.
- Hassani A, Khataee A, Karaca S, Fathinia M.** 2016. Heterogeneous photocatalytic ozonation of ciprofloxacin using synthesized titanium dioxide nanoparticles on a montmorillonite support: Parametric studies, mechanistic analysis and intermediates identification. Royal Society of Chemistry Advances **6**, 87569–87583.
- Yang J, Liang Q.** 2019. TiO₂/SiO₂ membrane materials via a sol–gel process: preparation and characterization calcined under N₂ atmosphere, Ferroelectrics, 547:1, 10-20.
- Joseph CG, Taufiq-Yap YH, Letshmanan E, Vijayan.** 2022. Heterogeneous photocatalytic chlorination of methylene blue using a newly synthesized TiO₂-SiO₂ photocatalyst. Catalysts **12(2)**, 156.
- Vardhan KH, Kumar PS, Panda RC.** 2019. A review on heavy metal pollution, toxicity and remedial measures: Current trends and future perspectives. Journal of Molecular Liquids **290**, 111197.
- Kumar PS.** 2021. Modern Treatment Strategies for Marine Pollution, Chapter One e Introduction to Marine Biology, pp. 1-10. DOI:10.1016/B978-0-12-822279-9.00008-7
- Malkappa K, Rao BN, Suresh G.** 2018. Organic/inorganic hybrid nanocolloids of water dispersible polyurethanes with antibacterial activity. Colloid Polymer Science **296**, 95–106.
- Villarín MC, Merel S.** 2020. Paradigm shifts and current challenges in wastewater management, Journal of Hazardous Materials **390**, 122139.
- Ruchianwar N, Bamne A, Singh J, Sharma N, Singh PK, Umar P, Haque A, Fozia.** 2022. Synthesis of titania/silica nanocomposite for enhanced photodegradation of methylene blue and methyl orange dyes under UV and mercury lights. Journal of Environmental Science Materials Manufacturing **16**, 2576-9898.
- YerliSoylu N, Soylyu A, Dikmetas DN, Karbancioglu-Guler F, Kucukbayrak S, ErolTaygun M.** 2023. Photocatalytic and Antimicrobial Properties of Electrospun TiO₂-SiO₂-Al₂O₃-ZrO₂-CaO-CeO₂ Ceramic Membranes ACS Omega **8(12)**, 10836-10850.
- Nabih S, Shalan AE, Abu Serea, ES, Goda MA, Sanad, MF.** 2019, Photocatalytic performance of TiO₂/SiO₂ nanocomposites for the treatment of different organic dyes, Journal of Material Science **3010**, 9623- 9633. Pages 2782-2799, ISSN 2213-3437,
- Palhares HG, Nunes EHM, Houmard M.** 2021. Heat treatment as a key factor for enhancing the photodegradation performance of hydrothermally-treated sol–gel TiO₂-SiO₂ nanocomposites. Journal of Sol-Gel Science and Technology **99**, 188–197.
- Parand P, Mohammadi M, Akmal AAS, samadpour M, Dehghani M, Parvazian E.** (2020). Sequential RTV/(TiO₂/SiO₂) nanocomposite deposition for suppressing the leakage current in silicone rubber insulators. Applied Physics A. **126(5)**.
- Prasannamedha G, Kumar PS, Mehala R, Sharumitha TJ, Surendhar D.** 2021. Enhanced adsorptive removal of sulfamethoxazole from water using biochar derived from hydrothermal carbonization of sugarcane bagasse. Journal of Hazard Materials **407**, 124825.
- Eddy DR, Ishmah SN, Permana MD, Firdaus ML.** 2020. Synthesis of titanium dioxide/silicon dioxide from beach sand as photocatalyst for Cr and Pb Remediation. Catalysts **10(11)**, 1248.

- Ranjbar M, Taher MA, Sam A.** 2016. Single-step synthesis of SiO₂-TiO₂ hydrophobic core-shell nanocomposite by hydrothermal method. *Journal of Cluster Science* **27**, 583–592.
- Rasouli F, Aber S, Salari D, Khataee AR.** 2014. Optimized removal of Reactive Navy Blue SP-BR by organo-montmorillonite based adsorbents through central composite design. *Applied Clay Science* **87**, 228–234.
- Ting Wang, Li Y, Wu W-T, Zhang Y-I, Wu L-G, Chen H-II.** 2021. Effect of chiral-arrangement on the solar adsorption of black TiO₂-SiO₂ mesoporous materials for photodegradation and photolysis, *Applied Surface Science* **537**, 148025.
- Mahanta U, Khandelwal M, Deshpande AS.** 2022. TiO₂@SiO₂ nanoparticles for methylene blue removal and photocatalytic degradation under natural sunlight and low-power UV light, *Applied Surface Science* **576**, Part A, 151745.
- Van Hung N, Nguyet BTM, Nghi NH, Nguyen VT, Binh TV, Tu NTT, Dung NN, Khieu DQ.** 2021. Visible light photocatalytic degradation of organic dyes using W-modified TiO₂/SiO₂ catalyst. *Vietnam Journal of Chemistry* **59**, 620-638.
- Waran P, Pp G.** 2016. Synthesis and characterization of TiO₂@SiO₂-Ag nanocomposites towards photocatalytic degradation of rhodamine B and methylene blue. *Journal of Material Science. Materials Electronics* **27(8)**.
- Zeng L, Sun H, Peng T, Lv X.** 2019. Comparison of the Phase Transition and Degradation of Methylene Blue of TiO₂, TiO₂/Montmorillonite Mixture and TiO₂/Montmorillonite Composite. *Frontier Chemistry* **7**, 538.